HHS Public Access

Author manuscript

Biomaterials. Author manuscript; available in PMC 2018 October 01.

Published in final edited form as:

Biomaterials. 2017 October ; 142: 31–40. doi:10.1016/j.biomaterials.2017.07.020.

Electrical preconditioning of stem cells with a conductive polymer scaffold enhances stroke recovery

Paul M. George[a,b,c,**], **Tonya M. Bliss**[b,c], **Thuy Hua**[b,c], **Alex Lee**[d], **Byeongtaek Oh**[a], **Alexa Levinson**[a], **Swapnil Mehta**[b], **Guohua Sun**[b,c], and **Gary K. Steinberg**[a,b,c,*]

[a]Department of Neurology, Stanford University School of Medicine, Stanford, CA, USA

[b]Department of Neurosurgery, Stanford University School of Medicine, Stanford, CA, USA

[c]Stanford Stroke Center and Stanford University School of Medicine, Stanford, CA, USA

[d]Department of Psychiatry, Stanford University School of Medicine, Stanford, CA, USA

Abstract

Exogenous human neural progenitor cells (hNPCs) are promising stroke therapeutics, but optimal delivery conditions and exact recovery mechanisms remain elusive. To further elucidate repair processes and improve stroke outcomes, we developed an electrically conductive, polymer scaffold for hNPC delivery. Electrical stimulation of hNPCs alters their transcriptome including changes to the VEGF-A pathway and genes involved in cell survival, inflammatory response, and synaptic remodeling. In our experiments, exogenous hNPCs were electrically stimulated (electrically preconditioned) via the scaffold 1 day prior to implantation. After *in vitro* stimulation, hNPCs on the scaffold are transplanted intracranially in a distal middle cerebral artery occlusion rat model. Electrically preconditioned hNPCs improved functional outcomes compared to unstimulated hNPCs or hNPCs where VEGF-A was blocked during *in vitro* electrical preconditioning. The ability to manipulate hNPCs via a conductive scaffold creates a new approach to optimize stem cell-based therapy and determine which factors (such as VEGF-A) are essential for stroke recovery.

Keywords

Conductive polymer; Stroke recovery; Neural stem cell; Electrical stimulation; Tissue engineering; Cell transplantation

[*]Corresponding author. Department of Neurosurgery, Stanford University School of Medicine, 300 Pasteur Drive R 281, Stanford, CA 94305-5327, USA. gsteinberg@stanford.edu (G.K. Steinberg). [**]Corresponding author. Department of Neurology and Neurological Sciences, Stanford University School of Medicine, 300 Pasteur Drive MC5778, Stanford, CA 94305-5778, USA. pgeorge1@stanford.edu (P.M. George).

Disclosure of potential conflicts of interest

Gary K. Steinberg serves in an advisory role for Peter Lazic US, Inc and has stock options in Qool Therapeutics and NeuroSave. The remaining authors have no conflicts of interest to declare with this work.

Appendix A. Supplementary data

Supplementary data related to this article can be found at http://dx.doi.org/10.1016/j.biomaterials.2017.07.020.

1. Introduction

Stroke remains a leading cause of morbidity and long-term disability [1]. While acute stroke treatments exist within a narrow time window, no approved medical therapies for stroke recovery are available [2,3]. Stem cells have emerged as a potential stroke therapeutic. Human neural progenitor cells (hNPCs) are a type of stem cell derived from embryonic cells to have a neural fate [4,5]. The critical mechanisms of action and optimal delivery methods of stem cells required for efficacy remain incompletely understood. The current thinking is that exogenous hNPCs likely improve functional outcomes through neurotrophic effects of secreted factors that increase synapse formation, angiogenesis, dendritic branching and new axonal projections, as well as modulating the immune system [6–9]. However, the precise molecular details remain to be elucidated.

Biomaterials offer a unique method to interact with stem cells and manipulate their properties. Biopolymers have provided protection for stem cells implanted into the harsh stroke milieu and increased survival [10,11]. Because previously studied polymers are not responsive to external stimuli (eg electrical stimulation), the environment is controlled by inherent properties of the polymer alone. Conductive polymers, on the other hand, provide a platform to interact with stem cells through electrical stimulation [12]. Unlike inert polymer scaffolds, conductive scaffolds allow for manipulation of the stem cells after seeding of cells on the scaffold. Electrical fields influence differentiation, ion channel density, and neurite outgrowth of stem cells and other cell types [13–15]. The effect of this stimulation on subsequent stem cell performance remains unexplored.

To allow for greater control and understanding of the optimal conditions for stem cell-enhanced stroke recovery, we have derived a scaffold made of the conductive polymer, polypyrrole (PPy), which has advantageous mechanical and conductive properties for neural implantation [16]. The conductive scaffold allows for *in vitro* electrical stimulation and subsequent implantation of hNPCs onto the peri-infarct cortex while on the scaffold. For this study, we electrically preconditioned hNPCs on the scaffold with a short period of electrical stimulation prior to implantation onto the cortical surface. Subsequently, the conductive scaffold carrying the hNPCs is removed from the cell chamber system and implanted intracranially using a minimally invasive method of simply placing the scaffold on the brain surface of stroke-injured rats. Using RNA sequencing (RNAseq) analysis we investigated changes in gene expression in the hNPCs induced by electrical stimulation and examined how the host rat brain responded to the stimulated hNPCs, to explore the molecular pathways of hNPC-induced post-stroke recovery. Furthermore, our results show that these electrically preconditioned hNPCs, with this novel transplantation paradigm, improve post-stroke neurologic function.

2. Materials and methods

2.1. Fabrication of the conductive scaffold system

PPy (Sigma-Aldrich, St. Louis, MO) was electroplated onto indium tin oxide (ITO) slides (Delta Technologies, Loveland, CO) as described previously [16]. After removal from the ITO, the conductive scaffold was clamped between pieces of polydimethylsiloxane (PDMS;

Sylgard, Dow, Auburn, MI) with a chamber slide forming cell chambers (Lab-Tek, Thermo Fisher, Waltham, MA; Fig. 1A). Wires were attached to the conductive scaffold outside of the chambers. For implantation, the cell chambers and PDMS were unclamped and separated from the conductive scaffold. Wires were also removed from the conductive scaffold prior to implantation. The dimensions of the implanted scaffolds were approximately 1 × 3 × 0.25 mm.

2.2. In vitro hNPC electrical stimulation

All stem cell procedures were approved by Stanford's Stem Cell Research Oversight committee. As previously described [17], hNPCs, passages 17–22, were used in these experiments and kept in DMEM-F12 media with 2% B27 and 1% N2 supplements along with LIF (10 μg/ml), EGF (20 μg/ml), and βFGF (10 ng/ml, all Invitrogen, Waltham, MA except for EGF and LIF from Millipore, Darmstadt, Germany). Briefly, the hNPCs were originally derived from the H9 human embryonic stem cell line (WiCell Research Institute). These cells were differentiated into hNPCs using serum free medium containing EGF, bFGF, and LIF. Cells were harvested from spheres that formed over multiple passages and upon passage 5–6 spheres were dissociated into a single cell suspension using trypsin-EDTA to form monolayers. In our previous work, these cells were further characterized to show that if the mitogenic factors were withheld, the hNPCs could differentiate into neurons, astrocytes, and oligodendrocytes (immunostaining at 10 days: Tuj1 62.5 ± 2.8%, Nestin 36.6 ± 2.7%, GFAP 1.9 ± 0.3%, and galactocerebrocide for oligodendrocytes 7.1 ± 0.4%) [17]. hNPCs were plated onto the PPy scaffold on Day 1 (125,000 cells/cm^2). On Day 2, media was changed for both electrically preconditioned and non-stimulated cell groups. Electrically preconditioned cells received a +1 V to −1 V square wave at 1 kHz for 1 h. The current was delivered through the PPy scaffold with wires attached to either side of the PPy scaffold outside of the cell chamber. For the bevacizumab (Avastin®, Genentech, San Francisco, CA) groups, bevacizumab was added to the media (0.5 mg/ml) 1 h before stimulation with the media changed on Day 2. The animals did not receive any bevacizumab. On Day 3, cells and supernatant were collected for analysis, or the PPy scaffold with or without hNPCs was washed with phosphate buffered saline (PBS) and implanted. The PPy scaffold-alone control samples were treated the same as the stimulated implants. For analysis of the duration of VEGF-A upregulation, cells were sampled on Day 5 and Day 7 for qPCR analysis.

2.3. In vitro immunostaining

In vitro immunostaining was performed on Day 3. Cell survival was determined by a Live/Dead kit (Life Technologies, Waltham, MA). Four random, representative 0.34 mm × 0.45 mm areas were analyzed, and alive and dead cells on the conductive scaffold were counted by a blinded-individual with results averaged across the four areas (cells/mm^2).

Cell differentiation was assessed with nestin, neuronal, glial, and oligodendrocyte markers. Primary antibodies were anti-Nestin (1:1000, Cat. ABD69, Millipore), anti βIII-tubulin (1:500, Neuromics, Edina, MN), anti-glial antifibrillary protein GFAP (1:500, Abcam, Cambridge, United Kingdom), and Anti-NG2 (1:500, Invitrogen). Secondary antibodies were from Life Technologies and DAPI (1:1000, Sigma-Aldrich). Four random,

representative 0.34 mm × 0.45 mm areas were analyzed, and a blinded individual counted total cell, glial cell, and neural cell markers.

2.4. RNA – seq

In vitro preconditioned and unstimulated hNPC cDNA was isolated 24 h following electrical stimulation as described above ($n = 4$ per group). Peri-infarct rat cortical tissue that was implanted with preconditioned or unstimulated cells ($n = 4$ per group) was excised on ice 3 weeks after stroke and treated with RNA*later* (Ambion, Thermo Fisher). RNA was extracted with the RNeasy Mini Plus kit (Qiagen, Hilden, Germany) after homogenization in Trizol (Life Technologies). cDNA was then synthesized as above and purity was verified by the Agilent BioAnalyzer system. A library was created and Illumina RNA sequencing was performed with paired runs by blinded individuals at the Stanford Functional Genomics Facility as described previously [18].

Reads were preprocessed with Trimmomatic (ver. 0.32) with FastQC (v0.11.2) for quality control. RNA-Seq data were processed with the Tophat/Cufflink pipeline as previously described [19]. Reads were mapped to whole genome using TopHat 2 (ver 2.0.1) with Bowtie2 indexes built from human (hg19) or rat (rn5). Gene annotations were constructed using GTF files downloaded from iGenomes with mean inner distances for each sample calculated using BBMap. Cufflink tools (ver. 2.2.1) were used to assemble and complete final statistical analysis.

2.5. RNA extraction and qPCR

For *in vitro* experiments, RNA extraction from hNPCs was performed using a Qiagen RNeasy Plus Micro Kit. The iScript cDNA Synthesis Kit (Bio-Rad, Hercules, CA) accomplished first-strand cDNA synthesis. The CFX96 Real-Time PCR detection system (Bio-Rad) was used to perform quantitative real-time PCR (qPCR). Taq polymerase and Taqman primers (Life Technologies) for Class I Beta-Tubulin (TUBB, Hs03929064), VEGF-A (Hs00900055), MMP-9 (Hs00234579), THBS1 (Hs00962908), TGFβ-1 (Hs00998133), and VEGF-B (Hs00173634) formed the qPCR reaction mixtures. The Delta-Delta CT method was utilized for qPCR analysis with the *TUBB* housekeeping gene and hNPCs grown on a glass chamber slide for 3 days as references.

2.6. ELISA VEGF-A and western blot analysis

Supernatant was collected from the hNPCs *in vitro*, on Day 3 after plating. A human VEGF-A ELISA kit (Thermo Fisher) was used to assess VEGF-A concentrations according to manufacturer instructions. Samples were performed in duplicate with $n = 4$ for each group. Western blot analysis was performed on stroked animals in the unstimulated and electrically preconditioned groups at Day 21 after stroke with anti-VEGF-A (1:500, AB46154, Abcam) as described previously [20].

2.7. dMCA occlusion and cell implantation

All animal procedures were approved by Stanford University's Administrative Panel on Laboratory Animal Care. Adult, male T-cell deficient nude rats (NIH-RNU 230 ± 30 g) [21] underwent distal middle cerebral artery (dMCA) occlusion model with occlusion of both

common carotid arteries lasting 30 min as described previously [22]. Rats were anesthetized with isoflurane with buprenorphine administered subcutaneously for analgesia. Ampicillin was in cage water 1 day prior to surgery (1 mg/ml) and for 7 days after transplantation.

One week after stroke, animals were randomized by vibrissae-whisker paw score, and implantation surgeries performed by a blinded individual. A craniectomy was drilled above the left cortex, and the dura opened. Conductive scaffolds (Day 3 after hNPC plating) from the *in vitro* system were implanted onto the rat cortex primarily on the penumbral cortex medial to the lesion (with approximately 5×10^4 cells in hNPC groups). Surgicel (Ethicon, Somerville, NJ) was placed over the implant to prevent movement with skin closure.

2.8. Stroke volume and slice immunohistochemistry

Rats were perfused and 40 μm coronal slices were sectioned. Primary antibodies were incubated overnight at 4 °C as described previously [22]: anti-β-dystroglycan (1:100, Abcam), anti-GFAP (1:500, Abcam), anti-βIII-tubulin (1:500, Neuromics). Secondary antibodies were added as above. Images were analyzed on a Zeiss optical microscope with Axiovision software.

In vivo survival of hNPCs was assessed 2 weeks post-implantation (3 weeks post-stroke). hNPCs were identified on the conductive scaffold after removal from the cortical surface by staining for human nuclei (1:250, Abcam). Four random, representative 0.34 mm × 0.45 mm areas were analyzed, and cells were counted by a blinded individual with results being averaged (cells/mm^2). To assess for hNPCs in the rat tissue, serial slices were taken 400 μm apart from the genu of the corpus collosum to the splenium. Human nuclei staining and counting were performed by a blinded observer.

Stroke volume was assessed using cresyl violet staining 5 weeks after stroke as described previously [22]. Serial slices were taken 400 μm apart from the genu of the corpus collosum to the splenium. Areas were calculated using the following equation $\frac{\text{Area\_Contralateral} - \text{Area\_Ipsilateral}}{\text{Area\_Contralateral}} \times 100$. Assessments were performed by a blinded individual.

2.9. Vessel density and bifurcation measurements

Blood vessels were labeled at 2 and 4 weeks after implantation with anti-β-dystroglycan antibodies as above [6]. Two representative peri-infarct areas (0.34 mm × 0.45 mm) were selected from each ipsilateral slice at 400-μm intervals from the genu of the corpus collosum to its splenium (resulting in generally 14–16 slices per animal). One of the areas evaluated is located in the peri-infarct area near the scaffold ~0.3 mm from the ventral surface, and the second is located more medially in the center of the peri-infarct area near the center of the stroke arc. These were selected at the same point in each slice by a blinded individual. ImageJ software was used by a blinded individual to calculate average vessel density and count bifurcation points. A bifurcation was defined as a division where subsequent vessels were smaller.

2.10. Behavior analysis

Animals were divided into matched groups based on pretransplant behavior testing (n = 12 per group) and behavior testing was performed by blinded individuals. Functional recovery was assessed using the modified neurologic severity scale (NSS) [23,24] (Supplementary Table 1) and the vibrissae-forepaw test [25]. Animals were trained on 3 separate days prior to recording their baseline behavior. After baseline, the animals underwent dMCA occlusion and were tested 1 week after stroke prior to implantation. Animals without a significant deficit (significant deficit = vibrissae-forepaw score prior to implantation at <30% of baseline) were removed.

2.11. Statistical analysis

Data was tested for normality and standard deviations using a normal quantile plot to determine the appropriate test (parametric vs non-parametric). Statistical evaluation was performed in Excel or with genomic software, and one-way ANOVA or a Kruskal-Wallis test followed by Mann-Whitney or student t - test was utilized to determine significance at $P < 0.05$. All tests were two-tailed unless performed as a confirmatory test. For RNA-Seq pathway analysis, a false discovery analysis was used to correct for multiple variables. Data are presented as mean ± SE.

3. Results

3.1. In vitro electrical stimulation of hNPCs via an electrically conductive scaffold system

We fabricated a unique, detachable conductive scaffold system for electrical stimulation of hNPCs (Fig. 1A). Because the components of the *in vitro* system are held together with reversible clamps, the conductive scaffold containing the seeded cells can be separated from the PDMS and cell chambers after *in vitro* stimulation for implantation. Initial studies showed that hNPCs could be effectively plated on our conductive scaffold system and stimulated with no change in cell survival at 1 day after stimulation (Fig. 1B and Supplementary Fig. 1A – B).

3.2. RNA expression changes in electrically preconditioned hNPCs

To understand the pathways changed by electrical stimulation, we evaluated how gene expression differed between unstimulated and electrically preconditioned hNPC groups using high throughput RNA-Seq. Looking at changes in the hNPCs, the *in vitro* experiments showed 1217 hNPC genes that were significantly altered by electrical preconditioning. Ingenuity pathway analysis (IPA) showed the most significant pathways changed included those with effects on cell cycle/proliferation, survival, gene expression, as well as cardiovascular development that includes angiogenesis (Table 1). Go term analysis also demonstrated modifications in multiple important angiogenesis, cell survival and proliferation pathways (Supplementary Table 2). To further identify important candidate genes, we analyzed genes that are the upstream regulators of pathways that were the most significantly modified between the two conditions. Three of the most significantly changed upstream regulators are key components of VEGF pathways that are important for angiogenesis, cell proliferation and plasticity (Fig. 2A, VEGF, VEGF-A, and HIF-1α [an

important regulator of VEGF]). We next looked at the genes that were present in all of the top 10 IPA pathways and were one of the most significant altered upstream regulators, and 5 genes were identified (*VEGF-A*, *TGFβ-1*, *HGF*, *RB1*, and *AGT*). Further examination of angiogenesis pathways found *VEGF-A*, as well as multiple genes that interact with the VEGF pathway, to be altered (Supplementary Table 3).

Because of the VEGF-A pathway's predominance in the analysis of the RNA-Seq data, VEGF-A was examined to illustrate the ability to identify important recovery mechanisms with our electrically conductive scaffold. Genes that were significantly altered in the VEGF-A pathway between the preconditioned and unstimulated hNPCs were determined (Fig. 2B). Currently, the main effect of stem cells is thought to be mediated through secreted factors, and to investigate this, VEGF-A and other secreted members of the pathway such as MMP-9 and THBS1 were chosen.

3.3. Electrical preconditioning alters hNPCs VEGF-A expression

To verify the role of VEGF-A in the improved efficacy of electrically preconditioned hNPCs, quantitative real-time qPCR was used to evaluate gene expression. VEGF-A expression in these cells was significantly increased compared to unstimulated cells on the conductive scaffold (Fig. 2C). Consistent with this, increased levels of VEGF-A protein were detected in the conditioned media from electrically preconditioned cells compared to that from unstimulated cells on the conductive scaffold (Fig. 2D). Moreover, the presence of bevacizumab (a human monoclonal antibody that blocks VEGF-A) during electrical preconditioning blocked the increase in *VEGF-A* gene expression (Fig. 2C) and secreted protein levels in the *in vitro* assay. Previous studies have shown a similar decrease in VEGF-A expression in the presence of bevacizumab and a mild stress [26]. The change in VEGF-A expression was transient with expression levels returning to baseline levels by Day 5 after preconditioning (Supplementary Fig. 2). Gene expression of other members of the *VEGF* family, such as *VEGF-B*, were not significantly altered by exposure to bevacizumab during electrical preconditioning (Supplementary Fig. 3).

MMP-9 gene expression, a protein in the VEGF-A pathway and involved in extracellular matrix remodeling and angiogenesis, was also augmented by electrical preconditioning (Fig. 2E). *THBS1* gene expression, another secreted member of the VEGF-A pathway, was not significantly changed. Additionally, transforming growth factor β-1 (*TGFβ-1*), while significantly changed between the electrically preconditioned and unstimulated hNPCs in the RNA-Seq data, did not show a significant difference with qPCR. *VEGF-B* gene expression, another member of the VEGF family, was not significantly changed with electrical preconditioning by qPCR or RNA-Seq analysis.

3.4. Electrically preconditioned hNPCs enhance stroke recovery

To determine how electrically stimulating hNPCs affects their ability to enhance stroke recovery, hNPCs on the conductive scaffold were electrically stimulated *in vitro* (preconditioned group) and 24 h later transplanted into stroke-injured rats (7 days post stroke) by placing the conductive scaffold containing the hNPCs on top of the cortical surface (Fig. 3A–C). The electrical connection was removed from the conductive scaffold

prior to implantation to prevent *in vivo* stimulation. Other experimental groups included animals that received the conductive scaffold with unstimulated hNPCs (unstimulated) and the conductive scaffold alone without hNPCs (polymer). Animals that received electrically preconditioned hNPCs (cells receiving *in vitro* electrical stimulation prior to implantation) experienced earlier and sustained improved recovery compared to the unstimulated group and the conductive scaffold alone control group as assessed by the Neurologic Severity Scale (NSS) (Fig. 3D). Utilizing the vibrissae-forepaw model, which primarily tests the sensorimotor/proprioceptive pathways, the electrically preconditioned group had earlier recovery, with the first significant difference observed at 3 weeks post-stroke (Fig. 3E). As expected, the unstimulated hNPC group also outperformed the polymer alone group but to a lesser extent than the preconditioned group in both the NSS and the vibrissae-forepaw test.

3.5. VEGF-A inhibition during electrical preconditioning reverses functional improvement

Because the RNA-Seq data showed VEGF-A to be an important factor changed with electrical preconditioning in our *in vitro* studies, we investigated whether treatment with bevacizumab during electrical preconditioning would prevent enhanced recovery. Bevacizumab was only applied to the cells during the *in vitro* time period, and the animals did not receive bevacizumab directly. Because VEGF-A was blocked only during the *in vitro* electrical preconditioning time period, we targeted the role of VEGF-A on the preconditioning effect and not subsequent VEGF-A expression of the cells *in vivo* after transplantation. Animals that received hNPCs with VEGF-A inhibition with or without electrical preconditioning lost the preconditioning effect and had the same recovery profile as the unstimulated hNPCs (Fig. 3D and E).

3.6. Electrical preconditioning increases peri-infarct vasculature in a VEGF-dependent manner

Because VEGF-A is significant in angiogenesis and has been linked to blood vessel density post-ischemia [27], peri-infarct vasculature was evaluated at two peri-infarct areas. One area was in close proximity to the conductive scaffold location at the cortical surface in the peri-infarct area, and the second was located in peri-infarct tissue more medially (Fig. 4A). Animals that received electrically preconditioned hNPCs had increased blood vessel density and numbers of vessel bifurcations in both regions compared to control groups (Fig. 4B–H). The vessel density changes were the same for both the area near the implant and the area in the middle of the peri-infarct area. This suggests that VEGF-A can act on medial areas of tissue that are further away from the cortical surface. By 5 weeks after stroke, the vasculature changes had normalized across all conditions as was seen in previous work (Supplementary Fig. 4) [6].

To further test the importance of the VEGF-A pathway on the electrical preconditioning effect, bevacizumab was applied to hNPCs during the *in vitro* electrical stimulation period (i.e. during the preconditioning step as mentioned above). hNPCs exposed to bevacizumab during the *in vitro* electrical preconditioning period did not increase blood vessel density or bifurcations following transplantation (Fig. 4E–H).

Multiple variables were evaluated to determine their effects on recovery. To insure that stroke volume was not a complicating factor, infarct size was measured and found to be similar between groups at 5 weeks after the stroke (Supplementary Fig. 5A–B). This was as expected given that the primary effect of the hNPCs delivered at 1 week post-stroke would be due to protection from secreted factors and not replacement of cells. Exposure to bevacizumab did not alter *in vitro* survival of hNPCs (Supplementary Fig. 6). Additionally, *in vivo* survival of the hNPCs on the conductive scaffolds themselves at 2 weeks did not change between different conditions (Supplementary Fig. 7). Although the main mechanism of recovery was thought to be the result of secreted factors, we evaluated for hNPCs in the parenchyma at 2 weeks post-transplantation (the time point where behavior was first significantly different) to determine ifhost integration of hNPCs could account for the effects we had seen. However, there was no appreciable survival of hNPCs observed in the brain parenchyma with immunofluorescent staining of hNPCs in the rat cortical tissue in any of the conditions. Because the stimulation period was brief, the electrical preconditioning did not change hNPC differentiation at the time of implantation. The cells remained largely undifferentiated with similar numbers of glial, neuronal, and oligodendrocyte precursors seen in both the electrically preconditioned and unstimulated groups as expected (Supplementary Fig. 8). The presence of bevacizumab also did not alter hNPC differentiation.

3.7. Electrical preconditioning alters rat cortical tissue

To determine the downstream effects of the electrically preconditioned cells on the rat cortex, the gene expression profiles of peri-infarct cortical tissue from rats who received electrically preconditioned hNPCs versus those with unstimulated hNPCs were also sequenced. The rat cortical tissue that received electrically preconditioned hNPCs had 528 genes whose expression significantly changed compared to rats that were implanted with unstimulated cells (Fig. 5A). These were fewer changes than observed in the hNPCs themselves where 1217 genes differed significantly (as described above). No human genes were observed in the rat cortical tissue analysis, indicating all of gene changes reflected alterations of the endogenous rat cortical tissue. Interestingly, the IPA pathways (Table 2) and Go term analysis (Supplementary Table 4) showed pathways involved with motor control and cortical remodeling were upregulated in the preconditioned group compared to animals receiving unstimulated cells, which one might expect when dealing with stroke recovery. None of the most significant pathways were related to cancer as seen in the hNPC pathways. Pathways important in cellular and synapse development and response to stimuli were modified in the rat cortex by the electrically preconditioned hNPCs. Of those genes that significantly changed, 42 genes were overlapping between the hNPCs and rat cortical tissue, indicating that common pathways in the hNPCs and downstream in the host cells are affected by electrical preconditioning (Supplementary Table 5).

VEGF-A was one of the genes significantly modified in both the hNPCs and rat cortex. Western analysis of the host rat cortex also verified an increase in rat VEGF-A in the animals that received electrically preconditioned hNPCs (Supplementary Fig. 9). Additionally, electrically preconditioned hNPCs altered 51 genes involved in angiogenesis in the host rat cortex, emphasizing the importance of angiogenesis in stem cell-enhanced stroke

recovery (Supplementary Table 6). Multiple genes downstream of *VEGF-A* were changed in the rat cortical tissue that received electrically preconditioned hNPCs, suggesting the importance of this mechanism in improved recovery (Fig. 5B).

4. Discussion

The ability to manipulate hNPCs seeded on a conductive scaffold provides a new platform to optimize hNPCs for stroke therapeutics as well as an innovative method to delineate critical pathways for stroke recovery. Electrically preconditioned hNPCs improved functional recovery after stroke. Numerous pathways were involved in hNPC-enhanced stroke recovery, and RNA-Seq results indicated that angiogenesis, cell proliferation and survival are integral processes in augmented repair. In our experiments, we demonstrated that electrical preconditioning changes gene expression in hNPCs, including those in the VEGF-A pathway, which is essential for enhanced recovery. The electrically preconditioned implanted hNPCs also modified the host rat cortex through secreted factors, causing changes to the endogenous vasculature and to gene expression involved in the VEGF-A pathway, motor functions, and cortical remodeling. If VEGF-A was blocked during *in vitro* electrical preconditioning, the functional and vasculature changes were lost.

Multiple pathways were changed with electrical preconditioning of the hNPCs as evidenced from the RNA-Seq and qPCR results. VEGF-A and MMP-9 are secreted factors that were modified with electrical preconditioning and have been shown to be important regulators of angiogenesis, cell survival, and stroke recovery [28–30]. Additionally, MMP-9 increases active VEGF during angiogenesis [31]. VEGF-A is known to be critical for stem cell-mediated stroke recovery [6], and prior studies indicate that overexpression of VEGF in hNPCs improves recovery [32,33]. Exogenous VEGF-A can increase endogenous VEGF-A production as well as its upstream regulator HIF-1α [34,35]. We believe this is the primary mechanism by which the VEGF-A pathways and vasculature are increased in the *in vivo* rat cortical tissue seen in our experiments, leading to improved recovery. Previously, it has been described that the vasculature changes driven by VEGF result in blood vessels with increased permeability [36]. Further studies of the observed vasculature changes could evaluate integrity of the vessels or determine if the increased vasculature has additional benefits for the behavioral improvement of the animals. Additional effects of VEGF-A after stroke would also be interesting to explore in future studies, including its role in the immune response and blood brain barrier regulation [37,38].

With our *in vitro* system, we can seed the hNPCs onto the conductive scaffold, stimulate the cells and then implant the conductive scaffold into the post-stroke environment. The novel transplantation method of placing the conductive polymer on the cortical surface would theoretically reduce injury associated with traditional intracranial transplantation methods requiring injection of cells into the brain parenchyma. Reduced transplantation injury could allow for easier clinical translation. Prior conductive scaffold systems, which allowed for *in vitro* stimulation of cells, were not able to form stand-alone conductive scaffolds suitable for *in vivo* implantation and cell delivery [12]. Our system's flexibility enables one to directly test the effect of electrical stimulation on the hNPCs without additional steps that might alter the cells (ie trypsinization). The conductive properties of PPy create the opportunity to

manipulate the cells after seeding on the conductive scaffold, which is not possible in previously described transplanted inert scaffolds. Additionally, as seen with inert polymer systems, the conductive scaffold provides protection from the harsh stroke environment, allowing a reduced number of cells to improve stroke recovery (300,000 hNPCs in previous methods [6] compared to 50,000 cells on the conductive scaffold). Reducing the number of stem cells needed to improve recovery could advance clinical translation given the limitations of a cell-based therapy dependent on a stable cell line, and the anticipated high demand for the treatment over many years.

Prior studies utilizing ischemia to precondition stem cells for stroke treatment have shown enhanced angiogenesis and neurogenesis with changes in the HIF-1α pathway, including VEGF and other trophic factors [39]. In our model, we suggest that the *in vitro* electrical preconditioning increases cytokine production; priming the hNPCs to improve function after stroke. Our preconditioning alters hNPC gene expression and factor release, thus improving the cells therapeutic potential. Similar to ischemia preconditioning studies, we found increased angiogenesis and regulation of the VEGF-A and HIF-1α pathways with electrical stimulation.

Electrically preconditioned cells improve the rate of recovery as well as enhance long-term function. Interestingly, in the vibrissae-forepaw test, which examines a more localized, sensorimotor pathway, the electrical preconditioning of cells led to a quicker recovery consistent with the concept that preconditioning optimizes cells to produce trophic factors more efficiently. With the NSS, a functional test incorporating multiple neuronal circuits, the rats with electrically preconditioned cells again improved more rapidly but continued to perform better throughout our testing, indicating a long-lasting effect of *in vitro* electrical preconditioning.

These studies support the theory that transplanted stem cells work through secreted factors that are able to act upon remote targets. Other possible mechanisms of recovery were not found in our model, with all groups having similar stroke volumes, hNPC survival, and differentiation at the time of transplantation. While alternative stem cell types such as mesenchymal stem cells also are known to work through secreted factors, hNPCs were thought to be more prepared to adapt to the neural environment given their differentiation to a neural fate [40].

We demonstrated that increased secreted VEGF-A by electrically preconditioned hNPCs is one pathway that enhances recovery. Vasculature changes occurred in the peri-infarct area near the implant as well as in tissue further from the scaffold. As the PPy scaffold was placed upon the cortical surface to reduce parenchymal injury and no hNPCs were observed within the parenchymal tissue, secreted factors produced by the stem cells likely are responsible for the improved stroke recovery. The fact that vessel changes were equivalent in areas both near and more distal to the hNPCs indicates that the secreted factors can effect tissue remote from the cells themselves. This allows for easier clinical translatability than direct implantation of isolated hNPCs into the peri-infarct area. Given the limitation of the small size of our rodent model, further studies are needed to determine if the larger distances in the human brain might reduce this effect.

The RNA-Seq experiments and western analysis demonstrate the downstream effects of electrically preconditioned hNPCs on the host cortex. While electrical preconditioning alters many hNPC genes involved in cellular division, survival and turnover; in the rat cortex that has received electrically preconditioned cells we do not see similar changes. In contrast, expression changes in the host cortex center on genes associated with neural movement circuits and cortical remapping as well as immune system changes. The VEGF-A pathway is also activated in rat cortical tissue, providing further evidence of its importance in recovery. As expected, multiple genes downstream of VEGF-A are modulated in the rat cortex by the electrical preconditioned hNPCs as seen in Fig. 5B, demonstrating the ability to modify the host response to ischemia through the use of electrically preconditioned hNPCs.

In the future, the electrical connections attached to the conductive scaffold during *in vitro* stimulation could be kept connected to the implanted scaffold. This would enable, via a cannula system, the conductive scaffold to be stimulated *in vivo*. This provides the ability to manipulate the implanted cells and cortex through continued electrical stimulation. Incorporating drugs or bioactive molecules into the conductive scaffold as shown previously [41] provides further control of the hNPCs and post-stroke environment. A biodegradable form of PPy could be used to limit the impact of a permanent scaffold remaining in the brain, which could help translate these findings to clinical applications. Additionally, because improvements in recovery rely on secreted factors, a cell-free system using biodegradable polymers for controlled release could theoretically be used to deliver the key factors [42].

Overall, electrically preconditioned hNPCs on a conductive polymer scaffold enhance stroke recovery. Multiple mechanisms are important for functional improvement after stroke with angiogenesis playing a crucial role in the improvement observed from electrical preconditioning. Our conductive scaffold allows us to manipulate hNPCs to optimize recovery and evaluate the important mechanisms for functional improvement, which has not been possible with prior non-polymeric or inert polymer implantation methods.

Supplementary Material

Refer to Web version on PubMed Central for supplementary material.

Acknowledgments

Funding

The work was supported in part by the American Brain Foundation/Academy of Neurology and NIH grant K08NS089976 to P.M.G; NIH grant RO1 N2058784, California Institute of Regenerative Medicine grant RB5-07363, Bernard and Ronni Lacroute, and the William Randolph Hearst Foundation to G.K.S.

We thank Eric Wang for blinding studies and Cindy H. Samos for manuscript assistance.

References

1. Go AS, Mozaffarian D, Roger VL, Benjamin EJ, Berry JD, Blaha MJ, Dai S, Ford ES, Fox CS, Franco S, Fullerton HJ, Gillespie C, Hailpern SM, Heit JA, Howard VJ, Huffman MD, Judd SE, Kissela BM, Kittner SJ, Lackland DT, Lichtman JH, Lisabeth LD, Mackey RH, Magid DJ, Marcus GM, Marelli A, Matchar DB, McGuire DK, Mohler ER 3rd, Moy CS, Mussolino ME, Neumar RW,

Nichol G, Pandey DK, Paynter NP, Reeves MJ, Sorlie PD, Stein J, Towfighi A, Turan TN, Virani SS, Wong ND, Woo D, Turner MB. Heart disease and stroke statistics–2014 update: a report from the american heart association. Circulation. 2014; 129(3):e28–e292. [PubMed: 24352519]

2. Tissue plasminogen activator for acute ischemic stroke. the national institute of neurological disorders and stroke rt-pa stroke study group. N. Engl. J. Med. 1995; 333(24):1581–1587. [PubMed: 7477192]
3. Grotta JC, Hacke W. Stroke neurologist's perspective on the new endovascular trials, stroke. J. Cereb. Circ. 2015; 46(6):1447–1452.
4. Reubinoff BE, Itsykson P, Turetsky T, Pera MF, Reinhartz E, Itzik A, Ben-Hur T. Neural progenitors from human embryonic stem cells. Nat. Biotechnol. 2001; 19(12):1134–1140. [PubMed: 11731782]
5. Zhang SC, Wernig M, Duncan ID, Brustle O, Thomson JA. In vitro differentiation of transplantable neural precursors from human embryonic stem cells. Nat. Biotechnol. 2001; 19(12):1129–1133. [PubMed: 11731781]
6. Horie N, Pereira MP, Niizuma K, Sun G, Keren-Gill H, Encarnacion A, Shamloo M, Hamilton SA, Jiang K, Huhn S, Palmer TD, Bliss TM, Steinberg GK. Transplanted stem cell-secreted vascular endothelial growth factor effects poststroke recovery, inflammation, and vascular repair. Stem Cell. Dayt. Ohio. 2011; 29(2):274–285.
7. Andres RH, Horie N, Slikker W, Keren-Gill H, Zhan K, Sun G, Manley NC, Pereira MP, Sheikh LA, McMillan EL, Schaar BT, Svendsen CN, Bliss TM, Steinberg GK. Human neural stem cells enhance structural plasticity and axonal transport in the ischaemic brain. Brain. J. Neurol. 2011; 134(6):1777–1789.
8. Chen J, Li Y, Wang L, Zhang Z, Lu D, Lu M, Chopp M. Therapeutic, benefit of intravenous administration of bone marrow stromal cells after cerebral ischemia in rats, stroke. J. Cereb. Circ. 2001; 32(4):1005–1011.
9. Daadi MM, Davis AS, Arac A, Li Z, Maag AL, Bhatnagar R, Jiang K, Sun G, Wu JC, Steinberg GK. Human neural stem cell grafts modify microglial response and enhance axonal sprouting in neonatal hypoxic-ischemic brain injury, stroke. J. Cereb. Circ. 2010; 41(3):516–523.
10. Bible E, Chau DY, Alexander MR, Price J, Shakesheff KM, Modo M. The support of neural stem cells transplanted into stroke-induced brain cavities by PLGA particles. Biomaterials. 2009; 30(16):2985–2994. [PubMed: 19278723]
11. Jin K, Mao X, Xie L, Galvan V, Lai B, Wang Y, Gorostiza O, Wang X, Greenberg DA. Transplantation of human neural precursor cells in Matrigel scaffolding improves outcome from focal cerebral ischemia after delayed postischemic treatment in rats. J. Cereb. Blood Flow Metabol. Official J. Int. Soc. Cereb. Blood Flow Metabol. 2010; 30(3):534–544.
12. Stewart E, Kobayashi NR, Higgins MJ, Quigley AF, Jamali S, Moulton SE, Kapsa RM, Wallace GG, Crook JM. Electrical stimulation using conductive polymer polypyrrole promotes differentiation of human neural stem cells: a biocompatible platform for translational neural tissue engineering. Tissue Eng. Part C. Methods. 2015; 4:385–393.
13. Chang KA, Kim JW, Kim JA, Lee SE, Kim S, Suh WH, Kim HS, Kwon S, Kim SJ, Suh YH. Biphasic electrical currents stimulation promotes both proliferation and differentiation of fetal neural stem cells. PLoS One. 2011; 6(4):e18738. [PubMed: 21533199]
14. Patel N, Poo MM. Orientation of neurite growth by extracellular electric fields. J. Neurosci. Official J. Soc. Neurosci. 1982; 2(4):483–496.
15. Prabhakaran MP, Ghasemi-Mobarakeh L, Jin G, Ramakrishna S. Electrospun conducting polymer nanofibers and electrical stimulation of nerve stem cells. J. Biosci. Bioeng. 2011; 112(5):501–507. [PubMed: 21813321]
16. George PM, Lyckman AW, LaVan DA, Hegde A, Leung Y, Avasare R, Testa C, Alexander PM, Langer R, Sur M. Fabrication and biocompatibility of polypyrrole implants suitable for neural prosthetics. Biomaterials. 2005; 26(17):3511–3519. [PubMed: 15621241]
17. Daadi MM, Maag AL, Steinberg GK. Adherent self-renewable human embryonic stem cell-derived neural stem cell line: functional engraftment in experimental stroke model. PLoS One. 2008; 3(2):e1644. [PubMed: 18286199]

18. Quail MA, Kozarewa I, Smith F, Scally A, Stephens PJ, Durbin R, Swerdlow H, Turner DJ. A large genome center's improvements to the Illumina sequencing system. Nat. Methods. 2008; 5(12): 1005–1010. [PubMed: 19034268]
19. Trapnell C, Roberts A, Goff L, Pertea G, Kim D, Kelley DR, Pimentel H, Salzberg SL, Rinn JL, Pachter L. Differential gene and transcript expression analysis of RNA-seq experiments with TopHat and Cufflinks. Nat. Protoc. 7(3):562–578.
20. Cheng MY, Wang EH, Woodson WJ, Wang S, Sun G, Lee AG, Arac A, Fenno LE, Deisseroth K, Steinberg GK. Optogenetic neuronal stimulation promotes functional recovery after stroke. Proc. Natl. Acad. Sci. 2014; 111(35):12913–12918. [PubMed: 25136109]
21. Vos JG, Kreeftenberg JG, Kruijt BC, Kruizinga W, Steerenberg P. The athymic nude rat. II. immunological. characterstics. Clin. Immunol. Immunopathol. 1980; 15(2):229–237. [PubMed: 6986220]
22. Kelly S, Bliss TM, Shah AK, Sun GH, Ma M, Foo WC, Masel J, Yenari MA, Weissman IL, Uchida N, Palmer T, Steinberg GK. Transplanted human fetal neural stem cells survive, migrate, and differentiate in ischemic rat cerebral cortex. Proc. Natl. Acad. Sci. U. S. A. 2004; 101(32):11839–11844. [PubMed: 15280535]
23. Chen J, Sanberg PR, Li Y, Wang L, Lu M, Willing AE, Sanchez-Ramos J, Chopp M. Intravenous administration of human umbilical cord blood reduces behavioral deficits after stroke in rats, stroke. J. Cereb. Circ. 2001; 32(11):2682–2688.
24. Garcia JH, Wagner S, Liu KF, Hu XJ. Neurological deficit and extent of neuronal necrosis attributable to middle cerebral artery occlusion in Statistical validation, rats, stroke. J. Cereb. Circ. 1995; 26(4):627–634. discussion 635.
25. Schallert T, Fleming SM, Leasure JL, Tillerson JL, Bland ST. CNS plasticity and assessment of forelimb sensorimotor outcome in unilateral rat models of stroke, cortical ablation, parkinsonism and spinal cord injury. Neuropharmacology. 2000; 39(5):777–787. [PubMed: 10699444]
26. Giurdanella G, Anfuso CD, Olivieri M, Lupo G, Caporarello N, Eandi CM, Drago F, Bucolo C, Salomone S. Aflibercept, bevacizumab and ranibizumab prevent glucose-induced damage in human retinal pericytes in vitro, through a PLA2/COX-2/VEGF-A pathway. Biochem. Pharmacol. 2015; 96(3):278–287. [PubMed: 26056075]
27. Zhang ZG, Zhang L, Jiang Q, Zhang R, Davies K, Powers C, Bruggen N, Chopp M. VEGF enhances angiogenesis and promotes blood-brain barrier leakage in the ischemic brain. J. Clin. Investig. 2000; 106(7):829–838.
28. Chang JJ, Emanuel BA, Mack WJ, Tsivgoulis G, Alexandrov AV. Matrix metalloproteinase-9: dual role and temporal profile in intracerebral hemorrhage. J. stroke Cerebrovasc. Dis. Official J. Natl. Stroke Assoc. 2014; 23(10):2498–2505.
29. Chun TH, Sabeh F, Ota I, Murphy H, McDonagh KT, Holmbeck K, Birkedal-Hansen H, Allen ED, Weiss SJ. MT1-MMP-dependent neovessel formation within the confines of the three-dimensional extracellular matrix. J. Cell. Biol. 2004; 167(4):757–767. [PubMed: 15545316]
30. Zhao BQ, Wang S, Kim HY, Storrie H, Rosen BR, Mooney DJ, Wang X, Lo EH. Role of matrix metalloproteinases in delayed cortical responses after stroke. Nat. Med. 2006; 12(4):441–445. [PubMed: 16565723]
31. Bergers G, Brekken R, McMahon G, Vu TH, Itoh T, Tamaki K, Tanzawa K, Thorpe P, Itohara S, Werb Z, Hanahan D. Matrix metalloproteinase-9 triggers the angiogenic switch during carcinogenesis. Nat. Cell. Biol. 2000; 2(10):737–744. [PubMed: 11025665]
32. Lee HJ, Kim KS, Park IH, Kim SU. Human neural stem cells over-expressing VEGF provide neuroprotection, angiogenesis and functional recovery in mouse stroke model. PLoS One. 2007; 2(1):e156. [PubMed: 17225860]
33. Miki Y, Nonoguchi N, Ikeda N, Coffin RS, Kuroiwa T, Miyatake S. Vascular endothelial growth factor gene-transferred bone marrow stromal cells engineered with a herpes simplex virus type 1 vector can improve neurological deficits and reduce infarction volume in rat brain ischemia. Neurosurgery. 2007; 61(3):586–594. discussion 594–5. [PubMed: 17881973]
34. Deudero JJ, Caramelo C, Castellanos MC, Neria F, Fernandez-Sanchez R, Calabia O, Penate S, Gonzalez-Pacheco FR. Induction of hypoxia-inducible factor 1alpha gene expression by vascular endothelial growth factor. J. Biol. Chem. 2008; 283(17):11435–11444. [PubMed: 18305118]

35. Knizetova P, Ehrmann J, Hlobilkova A, Vancova I, Kalita O, Kolar Z, Bartek J. Autocrine regulation of glioblastoma cell cycle progression, viability and radioresistance through the VEGF-VEGFR2 (KDR) interplay. Cell cycle Georget. Tex. 2008; 7(16):2553–2561.

36. Garcia-Roman J, Zentella-Dehesa A. Vascular permeability changes involved in tumor metastasis. Cancer Lett. 2013; 335:259–269. [PubMed: 23499893]

37. Manoonkitiwongsa PS, Schultz RL, Whitter EF, Lyden PD. Contraindications of VEGF-based therapeutic angiogenesis: effects on macrophage density and histology of normal and ischemic brains. Vasc. Pharmacol. 2006; 44(5):316–325.

38. Proescholdt MA, Heiss JD, Walbridge S, Muhlhauser J, Capogrossi MC, Oldfield EH, Merrill MJ. Vascular endothelial growth factor (VEGF) modulates vascular permeability and inflammation in rat brain. J. Neuropathol. Exp. Neurol. 1999; 58(6):613–627. [PubMed: 10374752]

39. Wei L, Fraser JL, Lu ZY, Hu X, Yu SP. Transplantation of hypoxia preconditioned bone marrow mesenchymal stem cells enhances angiogenesis and neurogenesis after cerebral ischemia in rats. Neurobiol. Dis. 2012; 46(3):635–645. [PubMed: 22426403]

40. Park DY, Mayle RE, Smith RL, Corcoran-Schwartz I, Kharazi AI, Cheng I. Combined transplantation of human neuronal and mesenchymal stem cells following spinal cord injury. Glob. Spine J. 2013; 3(1):1–6.

41. George PM, Saigal R, Lawlor MW, Moore MJ, LaVan DA, Marini RP, Selig M, Makhni M, Burdick JA, Langer R, Kohane DS. Three-dimensional conductive constructs for nerve regeneration. J. Biomed. Mater. Res. Part A. 2009; 91(2):519–527.

42. Pakulska MM, Tator CH, Shoichet MS. Local delivery of chondroitinase ABC with or without stromal cell-derived factor 1alpha promotes functional repair in the injured rat spinal cord. Biomaterials. 2017; 134:13–21. [PubMed: 28453954]

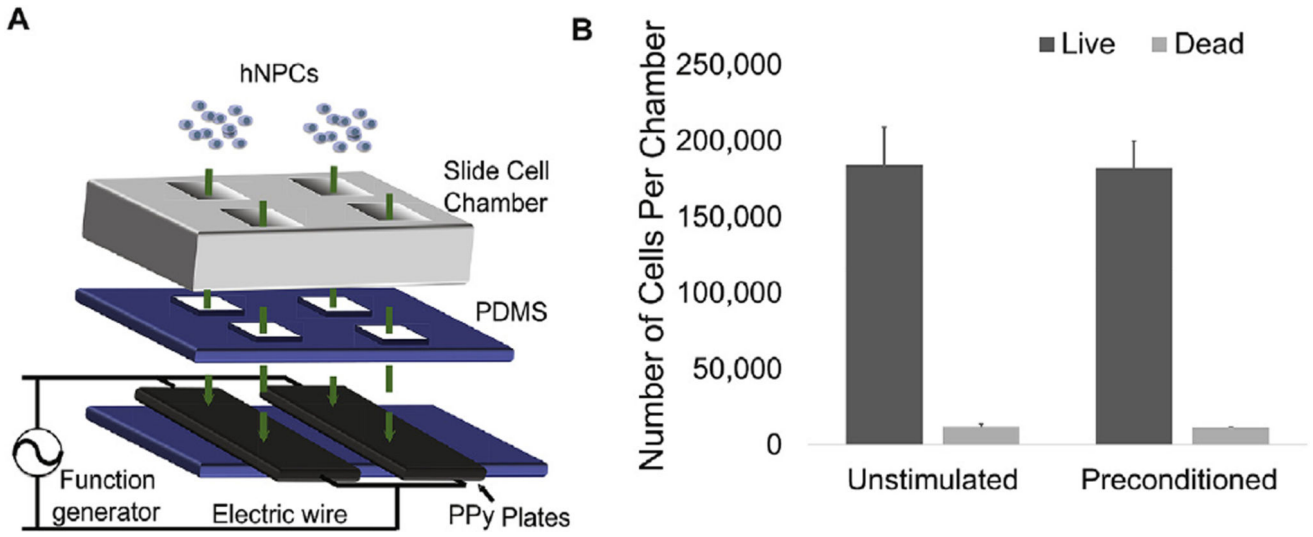

Fig. 1. In vitro PPy hNPC scaffold system for electrical stimulation

(A) Conductive scaffold system with hNPCs plating (PDMS, polydimethylsiloxane). (B) Live/dead assay results showing average number of living and dead cells (error bars show SE, n = 4, two-tailed Student *t*-test).

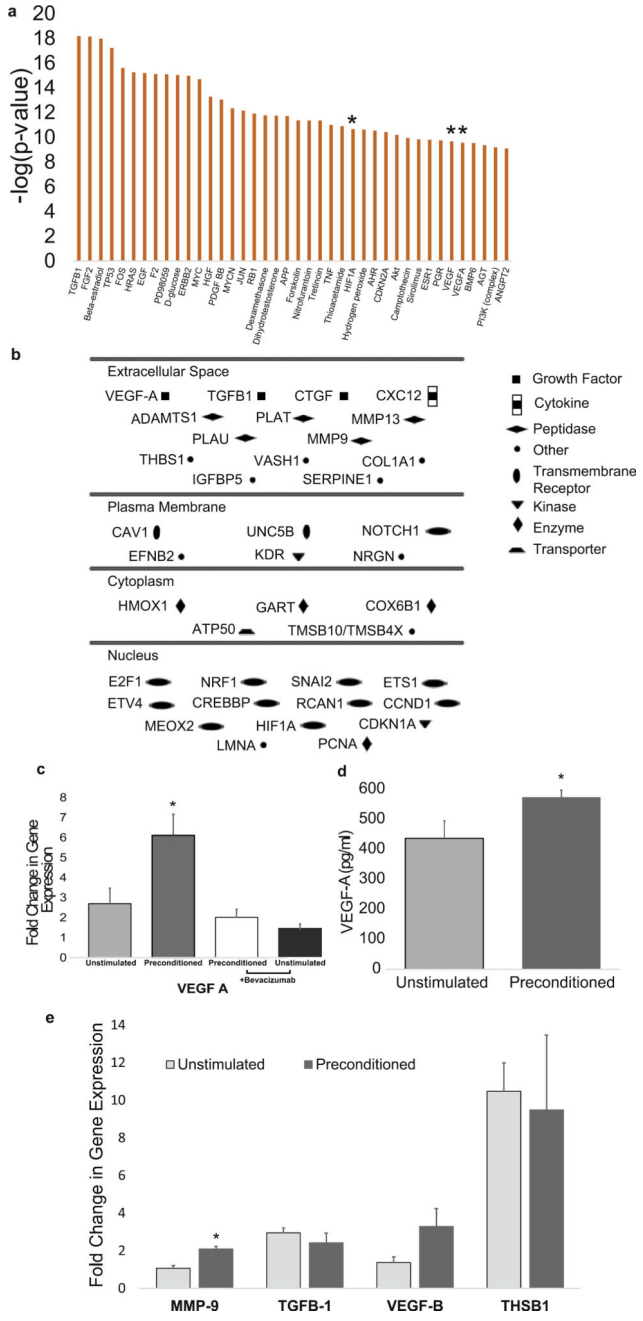

Fig. 2. Gene expression changes with electrical preconditioning

(A) Genes with the most significant downstream pathway changes in hNPCs (* indicates gene in VEGF pathway) (B) Schematic of significantly altered genes in the VEGF-A pathway and their location ($P < 0.05$ between stimulated and unstimulated groups after multiple comparison correction). (C) Fold change in gene expression of VEGF-A in hNPCs (* indicates difference $P < 0.05$ between electrically preconditioned and all other groups, error bars show SE, n = 4, two-tailed Mann-Whitney *U* test). (D) Concentration of VEGF-A secreted by hNPCs into supernatant (* indicates $P < 0.05$ from unstimulated, error bars show SE, n = 4, two-tailed Mann-Whitney *U* test). (E) Fold change in gene expression in hNPCs

(** indicates P < .01 from unstimulated, error bars show SE, n = 4, two-tailed Mann-Whitney *U* test).

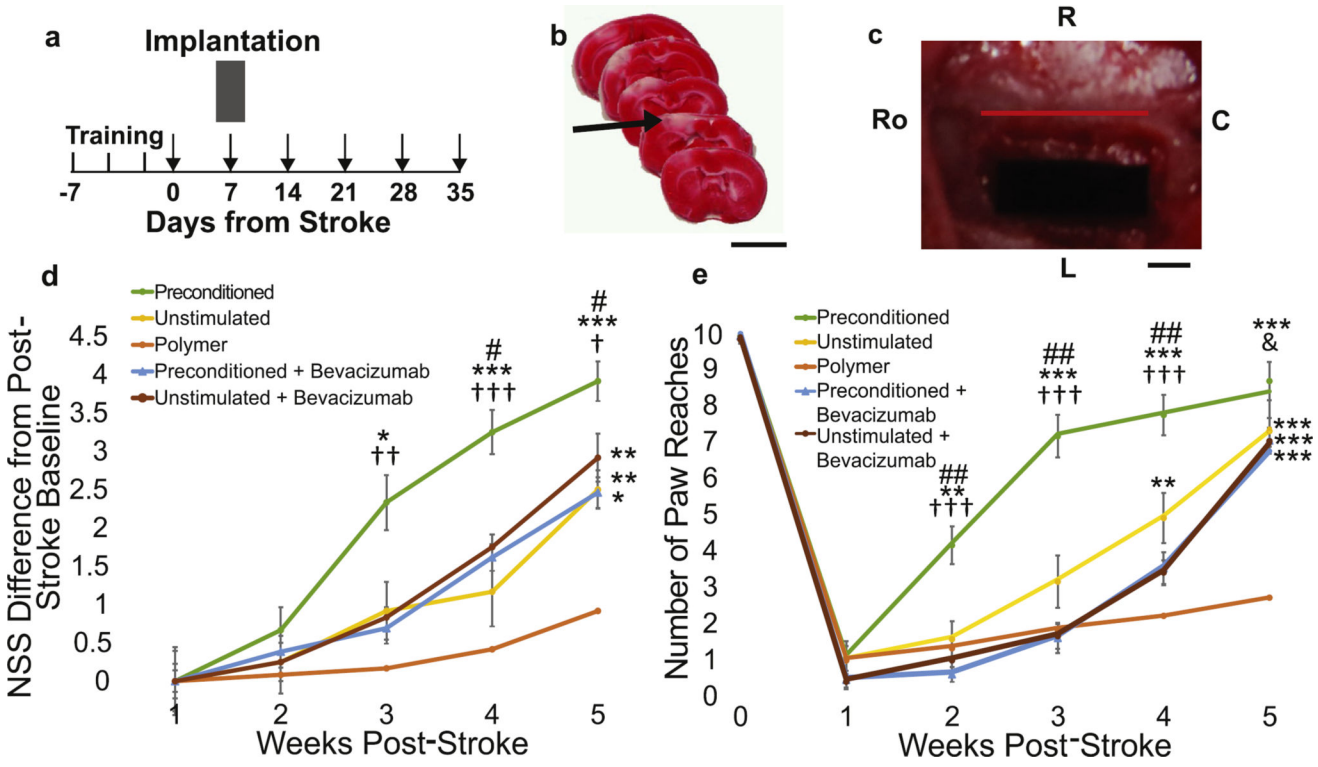

Fig. 3. Electrically preconditioned hNPC enhanced stroke recovery

(A) Experimental timeline with training occurring three times in the week prior to stroke and behavioral testing indicated by arrows. (B) 2,3,5-Triphenyltetrazolium chloride staining showing typical dMCA occlusion stroke (arrow indicates ischemic region in white, scale bar – 5 mm). (C) Conductive PPy scaffold implanted on cortical surface. (Ro – rostral; R – right; L – left; C – caudal, red bar indicates sagittal suture, scale bar – 1 mm). (D) Difference in Neurological Severity Scale (NSS) from post-stroke baseline. (E) Vibrissae-forepaw behavioral testing. (for (d) Kruskal-Wallis analysis of all groups showed 3 weeks post-stroke $H = 12.72$, $P = 0.013$, 4 weeks $H = 18.38$, $P = 0.001$, and 5 weeks $H = 23.70$, $P < 0.0001$ and (e) Kruskal-Wallis analysis showed at 2 weeks post-stroke $H = 20.33$, $P = 0.0004$, 3 weeks $H = 26.47$, $P < 0.0001$,4 weeks $H = 28.00$, $P < 0.0001$, and 5 weeks $H = 28.48$, $P \leq 0.0001$, post-hoc two-tailed Mann-Whitney *U* test shows * indicates $P < 0.05$ between group and polymer alone, ** indicates $P < 0.01$ between group and polymer alone, *** indicates $P < 0.001$ between group and polymer alone, # indicates $P < 0.05$ between group and unstimulated group, ## indicates $P < 0.01$ between group and unstimulated group, † indicates $P < 0.05$ between group and both bevacizumab groups, †† indicates $P < 0.01$ between group and both bevacizumab groups, ††† indicates $P < 0.001$ between group and both bevacizumab groups, & indicates $P < 0.05$ between group and stimulated bevacizumab group, error bars are SE, $n = 12$). (For interpretation of the references to colour in this figure legend, the reader is referred to the web version of this article.)

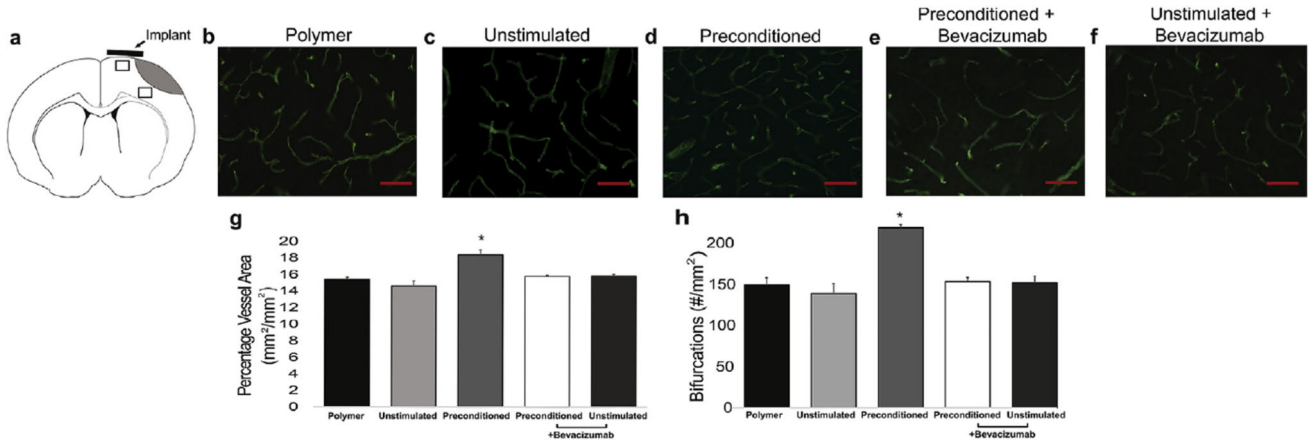

Fig. 4. Vasculature changes after stroke

(A) Schematic with areas for quantitative measurement indicated by rectangles. (B–F) Immunofluorescent β-dystroglycan staining of blood vessels (scale bar is 50 μm). (G) Quantitative measurements of percentage of blood vessel area (Kruskal-Wallis analysis showed H = 10.53, P = 0.015 with * indicate P < 0.05 between preconditioned cells and all other groups, n = 3, error bars show SE, two-tailed Mann-Whitney *U* test). (H) Quantitative measurements of blood vessel bifurcations (Kruskal-Wallis analysis showed H = 8.45, P = 0.040, * indicates P < 0.05 between preconditioned cells and all other groups, error bars show SE, n = 3, two-tailed Mann-Whitney *U* test).

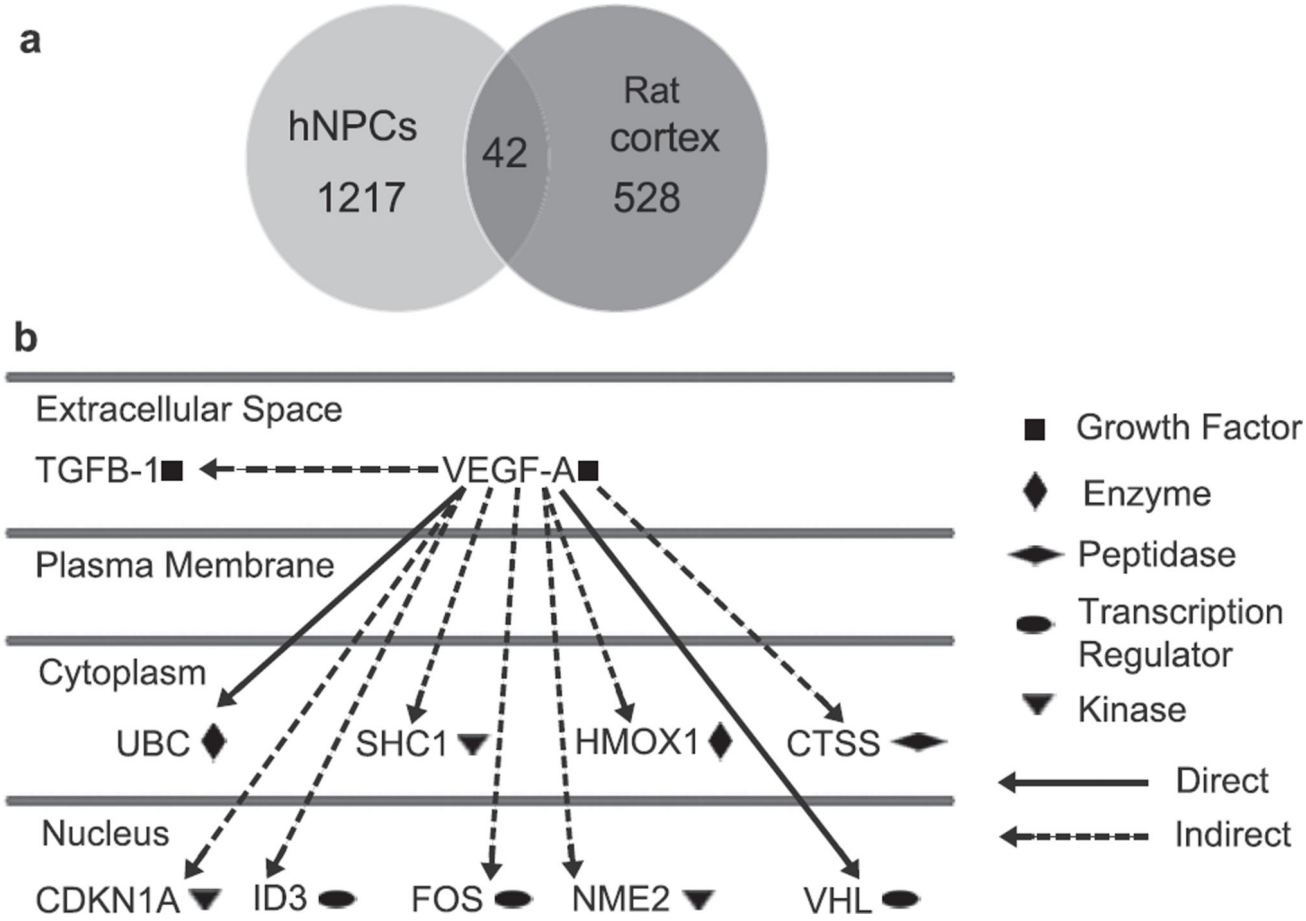

Fig. 5. Electrically preconditioned induced gene changes in rat cortex

(A) Venn diagram of gene expression changes in hNPCs (light gray) after electrical preconditioning and peri-infarct rat cortical tissue after hNPC transplantation (darker gray, $P < 0.05$ between stimulated and unstimulated groups after multiple comparison correction). (B) Significantly changed genes downstream of VEGF-A in the rat cortical tissue after transplantation and their locations.

Table 1

IPA results for the most significantly altered hNPC genes.

Disease and Functions	Range of p-values	# Molecules
Cancer	5.9E-32 – 3.95E-06	1065
Organismal Survival	1.33E-31 – 1.06E-09	366
Gene Expression	2.38E-27 – 5.02E-11	340
Cellular Growth and Proliferation	2.3E-25 – 3.62E-06	477
Cardiovascular System Development and Function	5.81E-25 – 1.89E-06	229

Table 2

IPA results for the most significantly altered rat cortical genes.

Disease and Functions	Range of p-values	# Molecules
Neurological Disease	2.33E-17 – 3.62E-03	169
Hereditary Disorder	1.07E-16 – 3.55E-03	77
Psychological Disorders	1.07E-16 – 3.34E-03	13
Skeletal and Muscular Disorders	4.85E-08 – 2.96E-03	116
Cellular Development	4.85E-08 – 3.04E-03	145